



Cite this: *J. Mater. Chem. A*, 2024, **12**, 28032

Aromatic pore surface with multiple adsorption sites for one-step C_2H_4 acquisition from C_2H_6/C_2H_4 mixture†

Yongqin Zhu,^{a,b} Zhenyu Ji,^{ab} Yunzhe Zhou^a and Mingyan Wu^{id, *acd}

Developing a C_2H_6 -selective adsorbent for the efficient one-step purification of C_2H_4 from C_2H_6/C_2H_4 mixture is of great significance but is still challenging because of the extremely close physicochemical properties of C_2H_6 and C_2H_4 . We herein report a metal–organic framework Ni-3-F, which possesses an aromatic pore surface and shows high-density distribution of N/O/F atoms on its pore wall. Such a special pore environment provides the C_2H_6 molecule with multitudinous binding sites. Adsorption experiments show that Ni-3-F exhibits a higher C_2H_6 adsorption capacity than C_2H_4 in the range of 273–313 K and delivers a high C_2H_6/C_2H_4 (1/99) selectivity of 1.80 at 298 K. Practical breakthrough experiments show that Ni-3-F can achieve efficient C_2H_6/C_2H_4 separation and realize a relatively high C_2H_4 yield (27.14 L kg⁻¹) at 298 K and 1 bar. Furthermore, according to its comparatively stable structure, Ni-3-F can maintain good separation performance at different temperatures (298–318 K), flow rates (1.05–2.95 mL min⁻¹) and relative humidities (33–100%). Computational simulations reveal that the aromatic pore surface and multiple N/O/F sites comprehensively provide C_2H_6 with more C–H···π and C–H···N/O/F supramolecular interactions, which allows Ni-3-F to preferentially adsorb C_2H_6 over C_2H_4 .

Received 22nd July 2024
 Accepted 26th August 2024

DOI: 10.1039/d4ta05086j
rsc.li/materials-a

Introduction

As the most important raw material in petrochemical industry, ethylene (C_2H_4) has been widely used for producing polyethylene, vinyl chloride, polyvinyl chloride and other chemicals.^{1–3} Until 2023, more than 200 million tons C_2H_4 had been produced by cracking petroleum hydrocarbons or pyrolysing ethane at high temperature.⁴ However, during the C_2H_4 production process, C_2H_6 is always inevitably produced as an impurity.^{5–7} In order to obtain polymer-grade C_2H_4 for its downstream applications, additional separation processes are required. Presently, in the industry, C_2H_4 is generally purified *via* cryogenic distillation at high pressure and low temperature, which not only requires exceedingly high equipment investment and complex operation processes, but is also extremely energy-intensive.^{8–10} The above purification technology cannot meet the requirements of sustainable and green development. Thus, a low-cost and high-efficiency separation method is urgently desired.

Adsorptive separation technology based on porous adsorbents has been deemed as a promising alternative. In recent years, with the boom in porous adsorbents, adsorptive separation technology has achieved rapid development and some significant separation processes, such as C_3H_8/C_3H_6 ,^{11–14} C_2H_2/CO_2 ,^{15–19} H_2/D_2 ,^{20–22} C_3F_6/C_3F_8 and so on,^{23,24} have been widely investigated. However, owing to the physical properties such as the molecular size, quadrupole moment and polarizability of C_2H_6 (4.4 Å, 0.65×10^{-26} esu cm² and 44.7×10^{-25} cm³, respectively), which are extremely close to those of C_2H_4 (4.2 Å, 1.5×10^{-26} esu cm² and 42.52×10^{-25} cm³, respectively), separating C_2H_6/C_2H_4 mixture is thus extraordinarily challenging.^{25,26} Furthermore, in order to directly acquire high-purity C_2H_4 from C_2H_6/C_2H_4 mixture, constructing a C_2H_6 -selective adsorbent is of great significance.^{5,27–29} According to the literature and our group's previous reports, designing porous materials with aromatic pores can efficiently enhance C_2H_6 adsorption through multiple C–H···π interactions.^{27,30,31} Moreover, in view of the more C–H bonds in the C_2H_6 molecule, inserting more electronegative groups such as nitrogen, oxygen and fluorine atoms in the framework can provide more C–H···N/O/F supramolecular interactions, which are helpful in increasing the uptake of C_2H_6 .³² Therefore, if we prepare a porous adsorbent with an aromatic pore surface and a high-density distribution of N/O/F binding sites in the pore wall, it may effectively realize preferential ethane adsorption and achieve high-efficiency C_2H_4 purification from C_2H_6/C_2H_4 mixture.

^aState Key Lab of Structure Chemistry, Fujian Institute of Research on the Structure of Matter, Chinese Academy of Sciences, Fuzhou 350002, China. E-mail: wumy@fjirs.ac.cn

^bCollege of Chemistry, Fuzhou University, Fuzhou, Fujian 350108, China

^cUniversity of Chinese Academy of Sciences, Beijing, 100049, China

^dFujian College, University of Chinese Academy of Sciences, Fuzhou, Fujian, 350002, China

† Electronic supplementary information (ESI) available: Experimental procedures. CCDC 2369828. For ESI and crystallographic data in CIF or other electronic format see DOI: <https://doi.org/10.1039/d4ta05086j>



Based on the above considerations, we herein employed a fluorinated organic ligand (3-fluoro-4-(pyridine-4-yl)benzoic acid) and constructed a novel quadruple interpenetrated MOF material (Ni-3-F). Benefiting from the high-density distribution of N/O/F atoms on its pore wall, Ni-3-F can provide multiple supramolecular bonding sites for C_2H_6 molecule, which makes it preferentially adsorb C_2H_6 rather than C_2H_4 . At 298 K and 1 bar, Ni-3-F can adsorb $77.44\text{ cm}^3\text{ g}^{-1}$ of C_2H_6 but can only absorb $65.13\text{ cm}^3\text{ g}^{-1}$ of C_2H_4 . Due to its different adsorption for C_2H_6 and C_2H_4 , Ni-3-F can efficiently capture C_2H_6 and provide high-purity C_2H_4 from the C_2H_6/C_2H_4 mixture (1/99, v/v). At 298 K and 1 bar, Ni-3-F can provide 27.14 L kg^{-1} of polymer-grade C_2H_4 from the C_2H_6/C_2H_4 mixture with a volume ratio of 1/99. More importantly, due to its high structural stability, Ni-3-F can even realize excellent C_2H_6/C_2H_4 separation at high temperature (313 K), high flow rate (2.95 mL min^{-1}) as well as high-humidity condition (100% relative humidity). Theoretical calculations show that Ni-3-F provides more supramolecular interactions with C_2H_6 than C_2H_4 , which is the key to realize efficient C_2H_6/C_2H_4 separation.

Experimental section

Materials and physical measurements

All chemicals were purchased from suppliers and used directly without further purification. 1H NMR spectra were recorded using a Bruker AVANCE III 400 (400 MHz) spectrometer. Single-crystal X-ray diffraction experiments were carried out on an XtaLAB Synergy R diffractometer. The powder X-ray diffraction (PXRD) data was recorded using a Rigaku MiniFlex600 X-ray diffractometer with Cu $K\alpha$ radiation ($\lambda = 1.5406\text{ \AA}$), scanning at 5° min^{-1} in the range of $4\text{--}50^\circ$. The sample was heated in air to the expected temperature and stored for about 10 min to collect PXRD patterns at different temperatures. The thermogravimetric analysis curves was recorded on an NETZSCH-STA-449C unit at a heating rate of $10\text{ }^\circ\text{C min}^{-1}$ in a nitrogen atmosphere.

Synthesis of ligand (3-fluoro-4-(pyridin-4-yl)benzoic acid)

The mixture of pyridin-4-ylboronic acid (3.7 g, 30 mmol), 4-bromo-3-fluorobenzoic acid (6.6 g, 30 mmol), Na_2CO_3 (8.5 g, 80 mmol) and $Pd(PPh_3)_4$ (2.4 g, 2.4 mmol) were dissolved in 130 mL H_2O and 150 mL 1,4-dioxane and heated to $105\text{ }^\circ\text{C}$ for 48 h under N_2 atmosphere. After the reaction was completed, the resulting mixture was cooled to room temperature and filtered. The solids were washed with ethanol ($3 \times 20\text{ mL}$) to collect the filtrate. Then, the filtrate was dried under vacuum condition. Finally, the filtrate was acidified using 3 M HCl to $pH = 3$ and then filtered. The solid was dried to obtain a white powder. The ligand purity was verified by 1H NMR. 1H NMR (400 MHz, $DMSO-d_6$): δ , 13.44 (s, 1H), 8.68–8.70 (m, 2H), 7.74–7.88 (m, 3H), 7.61–7.63 (m, 2H).

Synthesis of Ni-3-F

$Ni(NO_3)_2 \cdot 6H_2O$ (29.08 mg, 0.1 mmol) and 3-fluoro-4-(pyridin-4-yl)benzoic acid (21.72 mg, 0.1 mmol) were dissolved in 7.5 mL

DMF and 0.15 mL triethylamine. Then, they were transferred to a 25 mL Teflon-lined stainless-steel container and heated at $150\text{ }^\circ\text{C}$ for 3 days. After cooling, green block crystals could be obtained by filtering and washing multiple times with DMF.

Gas sorption experiment

All gas adsorption experiments were performed on an ASAP 3020 surface analyzer. Fresh samples were soaked in acetone for 7 days; during this time, fresh acetone was replaced 3 times each day. Before the adsorption experiments, the exchanged sample was treated in vacuum at room temperature for at least 6 hours. Then, in the adsorption tube, the sample was heated at $80\text{ }^\circ\text{C}$ for 10 hours with a high vacuum (less than $100\text{ }\mu\text{m Hg}$) to obtain activated Ni-3-F for the next adsorption tests. All adsorption experiments were carried out at liquid nitrogen temperature of 77 K or water bath temperature of $273\text{--}313\text{ K}$.

Breakthrough measurements

The breakthrough experiments were carried out by an HP-MC41 gas separation test system and a GC9860-5CNJ gas chromatograph. The breakthrough separation experiments for C_2H_6/C_2H_4 (1/99, v/v) were conducted in a fixed bed under ambient conditions. The sample column is a transparent quartz column with a length of 200 mm and an inner diameter of 3 mm. All gas flow rates are controlled by a mass flow controller, and gas flow rates outside the column are measured by a gas chromatography (GC) detector. The initially activated Ni-3-F crystal (sample mass: 1.1395 g) was tightly packed into the column and then activated for 10 hours at $80\text{ }^\circ\text{C}$ with Ar gas flow rate of 15 mL min^{-1} . In continuous cycle experiments, the sample was purified and regenerated by Ar purging at $80\text{ }^\circ\text{C}$ for 3 h.

Results and discussion

Crystal structure

Single crystal X-ray diffraction analysis shows that Ni-3-F crystallizes in the orthorhombic system and $Pnna$ space group. In the structure of Ni-3-F, the Ni(II) center adopts a tetra-coordination model, in which two pairs of pyridine and carboxyl groups from four neighboring 3-fluoro-4-(pyridin-4-yl)benzoic acid ligands are coordinated with the Ni(II) cation to form a 4-connected tetrahedral node (Fig. 1a). If simplifying the 3-fluoro-4-(pyridin-4-yl)benzoic acid ligand as a 2-connected linker, Ni-3-F possesses a 3D framework with specific *dia* topology (Fig. 1b). Additionally, in order to stabilize its structure, four independent frameworks interpenetrate with each other to form a 3D structure with 1D channel (Fig. 1c). The pore size is approximately 6.7 \AA (calculated by *zeo++* package) along the crystallographic *b*-axis (Fig. 1d and e). Furthermore, the porosity and the solvent-accessible pore volume void of Ni-3-F calculated by PLATON^{33,34} are 38.1% and 1214.76 \AA^3 , respectively. More importantly, despite the fourfold interpenetration, all the N/O/F atoms are distributed on the surface pore of Ni-3-F, which may provide more accessible binding sites for the C_2H_6 molecules.



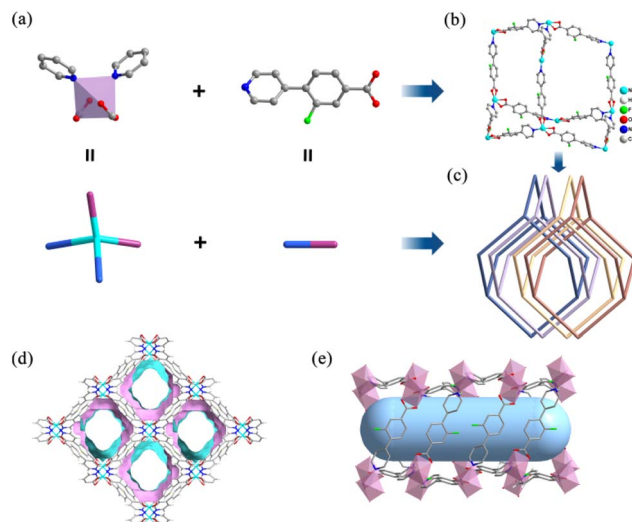


Fig. 1 (a) The coordination environment of Ni(II) ions in Ni-3-F. (b) The perspective view of a single set of a diamond network in Ni-3-F. (c) Four-fold interpenetrated *dia* nets in Ni-3-F. (d) The 1D channel viewed along the *b*-axis in Ni-3-F. (e) The rectangular 1D channel viewed along the *a*-axis.

Stability of Ni-3-F

The phase purity of Ni-3-F can be verified by powder X-ray diffraction (PXRD) experiments. As can be seen in Fig. S1,† the PXRD pattern of the as-synthesized sample matches well with the simulated ones. After Ni-3-F is soaked in common organic solvents, such as methanol, ethanol, acetone, acetonitrile and dichloromethane for 5 days, the PXRD patterns show that it can maintain its original structure (Fig. S2†). Furthermore, in order to determine its thermostability, thermogravimetric analysis (TGA) and variable temperature X-ray diffraction (VT-PXRD) experiments were conducted. As shown in Fig. S3,† there is no obvious weight loss until 350 °C. From the variable temperature X-ray diffraction (VT-PXRD) experiments (Fig. S4†), we find that the framework can be maintained at least up to 200 °C. The above results indicate that Ni-3-F has excellent structural stability, which can serve as a potential adsorbent in the actual industrial environment.

Gas sorption

On the basis of the structural stability and specially endowed channel, we conducted the gas adsorption tests for Ni-3-F. Firstly, the permanent porosity of Ni-3-F was established by N₂ adsorption experiments at 77 K. As seen in Fig. S5,† the 77 K N₂ isotherm exhibits reversible type-I adsorption behavior and the saturation adsorption capacity reaches 150.8 cm³ g⁻¹. The corresponding Brunauer–Emmett–Teller (BET) surface area is 583.4 m² g⁻¹. According to the abundance of F atoms and densely distributed N/O atoms on the pore wall, we speculate that Ni-3-F may generate stronger interaction for C₂H₆ molecule.^{35–39} In order to verify our hypothesis, we carried out single-component adsorption experiments for C₂H₆ and C₂H₄. As shown in Fig. 2a and b, the adsorption curves for C₂H₆ increase more sharply than those for C₂H₄ from 273 K to 313 K. At the same temperature, the

maximum adsorption capacity of C₂H₆ for Ni-3-F is always higher than that of C₂H₄. For example, at 298 K and 100 kPa, the uptake for C₂H₆ is 77.44 cm³ g⁻¹, which is higher than that of some reported C₂H₆-selective adsorbents, such as UIO-67 (67.42 cm³ g⁻¹),²⁷ Cu(Qc)₂ (41.5 cm³ g⁻¹),⁴⁰ ZIF-8 (56 cm³ g⁻¹)⁴¹ and FJI-H11-Me (58.0 cm³ g⁻¹)³⁰ but lower than that of some top-ranking materials, like Ni-MOF 2 (133 cm³ g⁻¹),⁴² MFM-300(Ind) (114.24 cm³ g⁻¹)¹³ and Co-9-ina (84.1 cm³ g⁻¹)³⁷ under the same conditions. In comparison, the uptake for C₂H₄ is only 65.13 cm³ g⁻¹. More importantly, in the low-pressure region, the adsorption isotherm for C₂H₆ also rises more sharply than that for C₂H₄, which indicates that Ni-3-F shows the stronger affinity for C₂H₆ (Fig. 2c). In order to investigate the cycle performance of Ni-3-F on C₂H₆ and C₂H₄, five continuous cycles of C₂H₆ and C₂H₄ adsorption experiments at 298 K were recorded. As seen in Fig. 2d and S6,† after five cycles, the C₂H₆ and C₂H₄ adsorption capacity show no obvious decrease.

In order to further assess the different interactions of C₂H₆ and C₂H₄, the heat of adsorption (Q_{st}) was calculated with adsorption isotherms at 273 K and 298 K. As shown in Fig. S7–S9,† the Q_{st} for C₂H₆ (25.47 kJ mol⁻¹) is much higher than that for C₂H₄ (21.09 kJ mol⁻¹) at zero coverage, implying that Ni-3-F indeed shows stronger interactions towards C₂H₆, which is beneficial for the preferential capture of C₂H₆ in the separation experiments. It is worth noting that compared with some known C₂H₆-selective adsorbents, such as JNU-2 (29.4 kJ mol⁻¹),⁴³ MUF-15 (29.2 kJ mol⁻¹),⁴⁴ Co-9-ina (30.6 kJ mol⁻¹),³⁷ Fe₂(O₂)(dobdc) (66.8 kJ mol⁻¹),⁴ PCN-250 (33.47 kJ mol⁻¹)²⁹ and Cu(Qc)₂ (28.8 kJ mol⁻¹),⁴⁰ the Q_{st} for C₂H₆ adsorption (25.47 kJ mol⁻¹) on Ni-3-F is lower. Such low Q_{st} highlights Ni-3-F as a promising C₂H₆-selective adsorbent with a low regenerative energy requirement.

In order to evaluate the adsorption selectivity for C₂H₆ and C₂H₄, an ideal adsorbed solution theory (IAST) calculation was employed on the basis of the single-component C₂H₆ and C₂H₄ adsorption isotherms at different temperatures (Fig. S10–S19†). As we can see from Fig. 2e, the adsorption selectivity for C₂H₆/C₂H₄ (1/99, v/v) at 298 K can reach 1.80, which is higher than that of some reported MOFs, such as In-soc-MOF-1 (1.4),⁴⁵ MIL-142A (1.5),⁴⁶ and Cu(ina)₂ (1.3).⁴⁰ More importantly, as the temperature increases, the IAST selectivities show no obvious decrease. Even at 313 K, the C₂H₆/C₂H₄ (1/99) selectivity can also climb to 1.69 at 1 bar, which indicates that Ni-3-F may achieve the separation of C₂H₆ and C₂H₄ at high temperature conditions. In order to further assess the separation ability of Ni-3-F for C₂H₆/C₂H₄, we calculated the separation potential (Δq) at different temperatures. As demonstrated in Fig. 2f, at 298 K and 1 bar, the Δq for C₂H₆/C₂H₄ (1/99) can reach 2.21 mmol g⁻¹. When the temperature rises to 313 K, the Δq can also be 1.45 mmol g⁻¹. All the above results collectively illustrate that Ni-3-F can not only realize the separation of C₂H₆ and C₂H₄ but give a high productivity of C₂H₄ in the separation process.

Theoretical mechanism calculations

In order to further explore the mechanism of Ni-3-F preferentially adsorbing C₂H₆ rather than C₂H₄, theoretical calculations



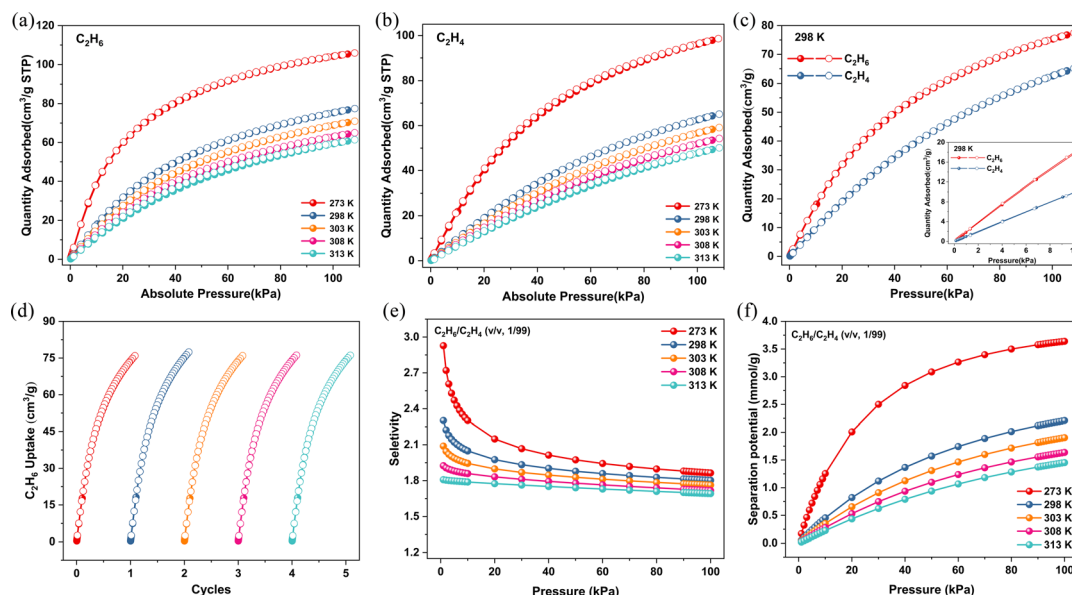


Fig. 2 Single-component adsorption isotherms of C_2H_6 (a) and C_2H_4 (b) in the range of 273–313 K. (c) The comparison of C_2H_6 and C_2H_4 isotherms for Ni-3-F at 298 K. (d) Five cycles of C_2H_6 adsorption isotherms at 298 K. (e) IAST selectivity and (f) separation potential for $\text{C}_2\text{H}_6/\text{C}_2\text{H}_4$ (1/99) at 273 K, 298 K, 303 K, 308 K and 313 K.

were carried out. As shown in Fig. 3, both C_2H_6 and C_2H_4 could form $\text{C}-\text{H}\cdots\text{F}$ and $\text{C}-\text{H}\cdots\pi$ interactions with the framework. However, it is found that the C_2H_4 molecule interacts with the framework only through $\text{C}-\text{H}\cdots\pi$ interactions (the separations between C and C atoms, 3.50–4.07 Å) and $\text{C}-\text{H}\cdots\text{F}$ interactions (the separations between H and F atoms, 2.66 Å) (Fig. 3a). By contrast, C_2H_6 has more interactions with the framework, including $\text{C}-\text{H}\cdots\pi$ interactions with benzene rings ($\text{C}\cdots\text{C}$ separations, 3.66–4.16 Å), $\text{C}-\text{H}\cdots\text{F}$ interactions with F atoms ($\text{H}\cdots\text{F}$ separations, 3.43 Å and 2.82 Å), $\text{C}-\text{H}\cdots\text{O}$ interactions between the carboxyl group ($\text{H}\cdots\text{O}$ separation, 3.39 Å), as well as $\text{C}-\text{H}\cdots\text{N}$ interactions with pyridine ($\text{H}\cdots\text{N}$, 2.91 Å and 3.15 Å) (Fig. 3b). The static binding energies of C_2H_6 and C_2H_4 are 48.48 and 42.40 kJ mol^{-1} , respectively, which is consistent with the experimentally observed abnormal affinity between the framework and the gas molecules. The above results show that the presence of multiple interaction sites can produce more

interaction between Ni-3-F and C_2H_6 , which is conducive to the one-step separation of $\text{C}_2\text{H}_6/\text{C}_2\text{H}_4$ to obtain high-purity C_2H_4 .

Column breakthrough tests

In order to verify the actual separation ability of Ni-3-F for $\text{C}_2\text{H}_6/\text{C}_2\text{H}_4$, we carried out breakthrough experiments in a packed bed with activated Ni-3-F sample. We used $\text{C}_2\text{H}_6/\text{C}_2\text{H}_4$ with a volume ratio of 1/99 to perform column breakthrough experiments. As shown in Fig. 4a, under the condition of 298 K and 1 bar, C_2H_4 always flows out of the fixed bed first, and after a certain time, C_2H_6 could be detected at the end of the fixed bed. The separation time of pure C_2H_4 is 28.8 min g^{-1} . According to the gas flow rate of 1.05 mL min^{-1} , after one separation cycle, about 27.14 L kg^{-1} polymer-grade C_2H_4 could be directly collected.

To the best of our knowledge, the adsorbent that may be applied in practical industry should have good durability. As depicted in Fig. 4b, after 5 cycles of breakthrough tests, the separation performance shows no significant decline, which proves that Ni-3-F has desirable repeatability and can serve as an ideal physical adsorbent in the industrial environment. As we know, the gas flow rates usually have an influence on gas separation. Therefore, the breakthrough experiments with different gas flow rates have also been investigated. As shown in Fig. 4c, when the gas flow rate gradually increases, Ni-3-F could still maintain excellent $\text{C}_2\text{H}_6/\text{C}_2\text{H}_4$ separation performance. Furthermore, in consideration of the high-temperature separation atmosphere in the industry and the inevitability of water vapor in the air, the adsorbent should also hold good separation ability in high temperature and high-humidity conditions. As shown in Fig. 4d, when the temperature is progressively enhanced, Ni-3-F could always realize one-step acquisition of high-purity C_2H_4 from the $\text{C}_2\text{H}_6/\text{C}_2\text{H}_4$ mixture. Even when the

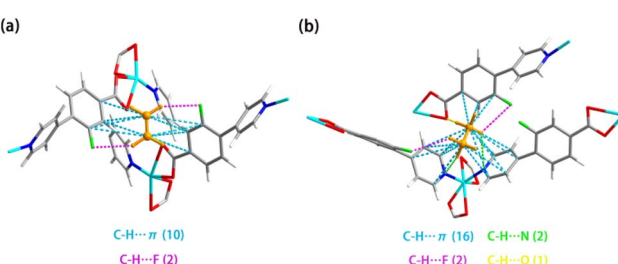


Fig. 3 Calculated preferential adsorption locations of C_2H_4 (a) and C_2H_6 (b) in Ni-3-F (the purple dotted line represents $\text{C}-\text{H}\cdots\text{F}$ interactions; the blue dotted line represents $\text{C}-\text{H}\cdots\pi$ interactions; the yellow dotted line represents $\text{C}-\text{H}\cdots\text{O}$ interactions; the green dotted line represents $\text{C}-\text{H}\cdots\text{N}$ interactions).

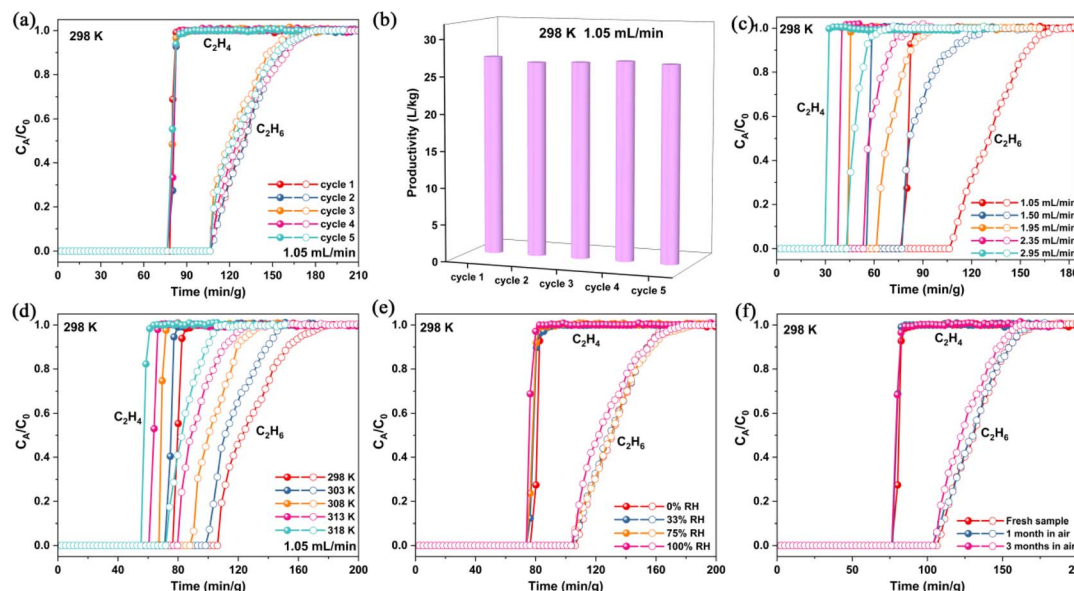


Fig. 4 Ni-3-F breakthrough experiments for $\text{C}_2\text{H}_6/\text{C}_2\text{H}_4$ (1/99, v/v). (a) Cyclic breakthrough tests of Ni-3-F for $\text{C}_2\text{H}_6/\text{C}_2\text{H}_4$ (1/99, v/v) with the flow rate of 1.05 mL min^{-1} . (b) Five-cycle C_2H_4 yields for $\text{C}_2\text{H}_6/\text{C}_2\text{H}_4$ (1/99, v/v) at 298 K and 1.05 mL min^{-1} . (c) Breakthrough experiments of Ni-3-F at 298 K with different flow rates. (d) Breakthrough experiments of Ni-3-F at different temperatures with a gas flow rate of 1.05 mL min^{-1} . (e) Breakthrough experiments of Ni-3-F under different relative humidity conditions and 298 K with a flow rate of 1.05 mL min^{-1} . (f) Breakthrough experiments of Ni-3-F after exposing to air for different time duration with a gas flow rate of 1.05 mL min^{-1} .

temperature increases to 318 K , 14.74 L kg^{-1} of C_2H_4 can be obtained. More importantly, when we introduce the moist $\text{C}_2\text{H}_6/\text{C}_2\text{H}_4$ mixture into the fixed bed, polymer-grade C_2H_4 can also be eluted out. As shown in Fig. 4e, the breakthrough curves in different humidity conditions could be coincident with that of the fresh sample, implying that the moisture has no effect on the separation of $\text{C}_2\text{H}_6/\text{C}_2\text{H}_4$. Moreover, Ni-3-F also exhibits excellent air stability, which can be demonstrated by the almost overlapping separation curves of the samples placed in air for 1 or 3 months with fresh samples (Fig. 4f). On the whole, the above results all show that Ni-3-F can realize the excellent separation of $\text{C}_2\text{H}_6/\text{C}_2\text{H}_4$ and can work well under various harsh conditions.

Conclusions

In summary, we have successfully prepared a four-fold interpenetrating MOF material (Ni-3-F), which has high-density of N/O/F atoms and realizes the preferential adsorption of C_2H_6 from $\text{C}_2\text{H}_6/\text{C}_2\text{H}_4$. At 298 K , the adsorption capacity of C_2H_6 ($77.44 \text{ cm}^3 \text{ g}^{-1}$) is significantly higher than that of C_2H_4 ($65.13 \text{ cm}^3 \text{ g}^{-1}$), and the selectivity of $\text{C}_2\text{H}_6/\text{C}_2\text{H}_4$ (1/99, v/v) can reach 1.80. The breakthrough experiments proved that high-purity C_2H_4 ($>99.95\%$) can be directly obtained from the mixture of $\text{C}_2\text{H}_6/\text{C}_2\text{H}_4$ (1/99, v/v) in one step, and the yield reaches 27.14 L kg^{-1} . More importantly, Ni-3-F can maintain good separation performance at different temperatures, flow rates and relative humidity conditions. The theoretical calculation results show that C_2H_6 can have a variety of interactions with the framework, and the interactions between Ni-3-F and C_2H_6 are obviously stronger than those of C_2H_4 . All the above results indicate that

the aromatic pore surface with multiple adsorption sites can successfully obtain high-purity C_2H_4 from the $\text{C}_2\text{H}_6/\text{C}_2\text{H}_4$ mixture in one step.

Data availability

All data included in this study are available upon request by contacting the corresponding author.

Author contributions

M. Y. W. determined the project. Y. Q. Z. and M. Y. W. designed the MOF synthesis methods. Y. Q. Z. and Z. Y. J. synthesized Ni-3-F. Y. Q. Z. and Y. Z. Z. carried out the power X-ray diffraction. Y. Q. Z. and Y. Z. Z. performed the single-crystal X-ray diffraction experiments. Y. Q. Z. and Z. Y. J. collected data of single-component gas sorption measurements and dynamic breakthrough experiments. Y. Q. Z. wrote the manuscript with support from M. Y. W. All authors contributed to revise the manuscript.

Conflicts of interest

There are no conflicts to declare.

Acknowledgements

This work is supported by NSFC (22271282) and the Self-deployment Project Research Program of Haixi Institutes, Chinese Academy of Sciences with the grant number of CXZX-2022-JQ04. Additionally, this work is also supported by Fujian



Science & Technology Innovation Laboratory for Optoelectronic Information of China (No. 2021ZR120) and NSF of Fujian Province (No. 2021J01517 and 2020J06034).

Notes and references

- 1 K. H. Cho, J. W. Yoon, J. H. Lee, J. C. Kim, D. Jo, J. Park, S.-K. Lee, S. K. Kwak and U. H. Lee, Design of Pore Properties of an Al-Based Metal-Organic Framework for the Separation of an Ethane/Ethylene Gas Mixture *via* Ethane-Selective Adsorption, *ACS Appl. Mater. Interfaces*, 2023, **15**, 30975–30984.
- 2 X. Lin, Y. Yang, X. Wang, S. Lin, Z. Bao, Z. Zhang and S. Xiang, Functionalized metal-organic and hydrogen-bonded organic frameworks for C_2H_4/C_2H_6 separation, *Sep. Purif. Technol.*, 2024, **330**, 125252.
- 3 S.-M. Wang, M. Shivanna, S.-T. Zheng, T. Pham, K. A. Forrest, Q.-Y. Yang, Q. Guan, B. Space, S. Kitagawa and M. J. Zaworotko, Ethane/Ethylene Separations in Flexible Diamondoid Coordination Networks *via* an Ethane-Induced Gate-Opening Mechanism, *J. Am. Chem. Soc.*, 2024, **146**, 4153–4161.
- 4 L. Li, R.-B. Lin, R. Krishna, H. Li, S. Xiang, H. Wu, J. Li, W. Zhou and B. Chen, Ethane/ethylene separation in a metal-organic framework with iron-peroxo sites, *Science*, 2018, **362**, 443–446.
- 5 K. Zhang, J.-J. Pang, X. Lian, Z.-H. Song, Y.-C. Yuan, H. Huang, Z.-Q. Yao and J. Xu, A pacs-type metal-organic framework with high adsorption capacity for inverse C_2H_6/C_2H_4 separation, *New J. Chem.*, 2024, **48**, 10577–10583.
- 6 L. Zhang, L. Li, E. Hu, L. Yang, K. Shao, L. Yao, K. Jiang, Y. Cui, Y. Yang, B. Li, B. Chen and G. Qian, Boosting Ethylene/Ethane Separation within Copper(I)-Chelated Metal-Organic Frameworks through Tailor-Made Aperture and Specific π -Complexation, *Adv. Sci.*, 2020, **7**, 1901918.
- 7 D. Lv, P. Zhou, J. Xu, S. Tu, F. Xu, J. Yan, H. Xi, W. Yuan, Q. Fu, X. Chen and Q. Xia, Recent advances in adsorptive separation of ethane and ethylene by C_2H_6 -selective MOFs and other adsorbents, *Chem. Eng. J.*, 2022, **431**, 133208.
- 8 A. Noonikara-Poyil, H. Cui, A. A. Yakovenko, P. W. Stephens, R. B. Lin, B. Wang, B. Chen and H. V. R. Dias, A Molecular Compound for Highly Selective Purification of Ethylene, *Angew. Chem., Int. Ed.*, 2021, **60**, 27184–27188.
- 9 Z. Di, X. Zheng, Y. Qi, H. Yuan and C.-P. Li, Recent Advances in C2 Gases Separation and Purification by Metal-Organic Frameworks, *Chin. J. Struct. Chem.*, 2022, **41**, 2211031–2211044.
- 10 S. Mukherjee, D. Sensharma, K.-J. Chen and M. J. Zaworotko, Crystal engineering of porous coordination networks to enable separation of C2 hydrocarbons, *Chem. Commun.*, 2020, **56**, 10419–10441.
- 11 Y. Wang, N. Y. Huang, X. W. Zhang, H. He, R. K. Huang, Z. M. Ye, Y. Li, D. D. Zhou, P. Q. Liao, X. M. Chen and J. P. Zhang, Selective Aerobic Oxidation of a Metal-Organic Framework Boosts Thermodynamic and Kinetic Propylene/Propane Selectivity, *Angew. Chem., Int. Ed.*, 2019, **58**, 7692–7696.
- 12 Z. Zhang, Q. Ding, X. Cui, X.-M. Jiang and H. Xing, Fine-Tuning and Selective-Binding within an Anion-Functionalized Ultramicroporous Metal-Organic Framework for Efficient Olefin/Paraffin Separation, *ACS Appl. Mater. Interfaces*, 2020, **12**, 40229–40235.
- 13 L. Guo, M. Savage, J. H. Carter, X. Han, I. da Silva, P. Manuel, S. Rudić, C. C. Tang, S. Yang and M. Schröder, Direct Visualization of Supramolecular Binding and Separation of Light Hydrocarbons in MFM-300(In), *Chem. Mater.*, 2022, **34**, 5698–5705.
- 14 Y. Wang, T. Li, L. Li, R. B. Lin, X. Jia, Z. Chang, H. M. Wen, X. M. Chen and J. Li, Construction of Fluorinated Propane-Trap in Metal-Organic Frameworks for Record Polymer-Grade Propylene Production under High Humidity Conditions, *Adv. Mater.*, 2023, **35**, 2207955.
- 15 X. Mu, Y. Xue, M. Hu, P. Zhang, Y. Wang, H. Li, S. Li and Q. Zhai, Fine-tuning of pore-space-partitioned metal-organic frameworks for efficient C_2H_2/C_2H_4 and C_2H_2/CO_2 separation, *Chin. Chem. Lett.*, 2023, **34**, 107296.
- 16 H. Li, C. Chen, Z. Di, Y. Liu, Z. Ji, S. Zou, M. Wu and M. Hong, Rational Pore Design of a Cage-like Metal-Organic Framework for Efficient C_2H_2/CO_2 Separation, *ACS Appl. Mater. Interfaces*, 2022, **14**, 52216–52222.
- 17 H. Li, C. Liu, C. Chen, Z. Di, D. Yuan, J. Pang, W. Wei, M. Wu and M. Hong, An Unprecedented Pillar-Cage Fluorinated Hybrid Porous Framework with Highly Efficient Acetylene Storage and Separation, *Angew. Chem., Int. Ed.*, 2021, **60**, 7547–7552.
- 18 M. Guo, Z. Jiang, S. Wu, C. Zhang, S. Zhu, L. Li, H. Zhang, L. Liu, S. Xiang and Z. Yao, Auxiliary ligand influence on interpenetration and C_2H_2/CO_2 separation in NDI based isoreticular MOFs, *Inorg. Chem. Commun.*, 2024, **165**, 112578.
- 19 K. Jiang, Y. Gao, P. Zhang, S. Lin and L. Zhang, A new perchlorate-based hybrid ultramicroporous material with rich bare oxygen atoms for high C_2H_2/CO_2 separation, *Chin. Chem. Lett.*, 2023, **34**, 108039.
- 20 F. Banijamali, A. Maghari, G. Schutz and M. Hirscher, Hydrogen and deuterium separation on metal organic frameworks based on Cu- and Zn-BTC: an experimental and theoretical study, *Adsorption*, 2021, **27**, 925–935.
- 21 F. Wu, L. Li, Y. Tan, E.-S. M. El-Sayed and D. Yuan, The competitive and synergistic effect between adsorption enthalpy and capacity in D_2/H_2 separation of $M_2(m\text{-dobdc})$ frameworks, *Chin. Chem. Lett.*, 2021, **32**, 3562–3565.
- 22 J. Teufel, H. Oh, M. Hirscher, M. Wahiduzzaman, L. Zhechkov, A. Kuc, T. Heine, D. Denysenko and D. Volkmer, MFU-4-A Metal-Organic Framework for Highly Effective H_2/D_2 Separation, *Adv. Mater.*, 2012, **25**, 635–639.
- 23 W. Xia, Y. Yang, L. Sheng, Z. Zhou, L. Chen, Z. Zhang, Z. Zhang, Q. Yang, Q. Ren and Z. Bao, Temperature-dependent molecular sieving of fluorinated propane/propylene mixtures by a flexible-robust metal-organic framework, *Sci. Adv.*, 2024, **10**, eadj6473.
- 24 M. Zheng, W. Xue, T. Yan, Z. Jiang, Z. Fang, H. Huang and C. Zhong, Fluorinated MOF-Based Hexafluoropropylene Nanotrap for Highly Efficient Purification of



- Octafluoropropane Electronic Specialty Gas, *Angew. Chem., Int. Ed.*, 2024, **136**, e202401770.
- 25 B. Zhu, J.-W. Cao, S. Mukherjee, T. Pham, T. Zhang, T. Wang, X. Jiang, K. A. Forrest, M. J. Zaworotko and K.-J. Chen, Pore Engineering for One-Step Ethylene Purification from a Three-Component Hydrocarbon Mixture, *J. Am. Chem. Soc.*, 2021, **143**, 1485–1492.
- 26 H. Shuai, J. Liu, Y. Teng, X. Liu, L. Wang, H. Xiong, P. Wang, J. Chen, S. Chen, Z. Zhou, S. Deng and J. Wang, Pillar-layered metal-organic frameworks with benchmark C_2H_2/C_2H_4 and C_2H_6/C_2H_4 selectivity for one-step C_2H_4 production, *Sep. Purif. Technol.*, 2023, **323**, 124392.
- 27 Y. Han, L. Liu, Z. Han and M. Wu, Engineering ethane-trapping metal-organic framework for efficient ethylene separation under high humid conditions, *Sep. Purif. Technol.*, 2024, **342**, 127011.
- 28 L. Yang, Q. Gao, Y.-M. Zhang, R. Wang and L.-Z. Chen, Efficient C_2H_6/C_2H_4 adsorption separation by a microporous heterometal-organic framework, *J. Colloid Interface Sci.*, 2023, **652**, 1093–1098.
- 29 Y. Chen, Z. Qiao, H. Wu, D. Lv, R. Shi, Q. Xia, J. Zhou and Z. Li, An ethane-trapping MOF PCN-250 for highly selective adsorption of ethane over ethylene, *Chem. Eng. Sci.*, 2018, **175**, 110–117.
- 30 Z. Di, C. Liu, J. Pang, S. Zou, Z. Ji, F. Hu, C. Chen, D. Yuan, M. Hong and M. Wu, A Metal-Organic Framework with Nonpolar Pore Surfaces for the One-Step Acquisition of C_2H_4 from a C_2H_4 and C_2H_6 Mixture, *Angew. Chem., Int. Ed.*, 2022, **61**, e202210343.
- 31 Y. Zhou, C. Chen, R. Krishna, Z. Ji, D. Yuan and M. Wu, Tuning Pore Polarization to Boost Ethane/Ethylene Separation Performance in Hydrogen-Bonded Organic Frameworks, *Angew. Chem., Int. Ed.*, 2023, **62**, e202305041.
- 32 G.-D. Wang, H.-H. Wang, W.-J. Shi, L. Hou, Y.-Y. Wang and Z. Zhu, A highly stable MOF with F and N accessible sites for efficient capture and separation of acetylene from ternary mixtures, *J. Mater. Chem. A*, 2021, **9**, 24495–24502.
- 33 A. L. Spek, Structure validation in chemical crystallography, *Acta Crystallogr., Sect. D: Biol. Crystallogr.*, 2009, **65**, 148–155.
- 34 A. L. Spek, Single-crystal structure validation with the program PLATON, *J. Appl. Crystallogr.*, 2003, **36**, 7–13.
- 35 C. X. Chen, Z. W. Wei, T. Pham, P. C. Lan, L. Zhang, K. A. Forrest, S. Chen, A. M. Al-Enizi, A. Nafady, C. Y. Su and S. Ma, Nanospace Engineering of Metal-Organic Frameworks through Dynamic Spacer Installation of Multifunctionalities for Efficient Separation of Ethane from Ethane/Ethylene Mixtures, *Angew. Chem., Int. Ed.*, 2021, **60**, 9680–9685.
- 36 L. Yang, L. Yan, W. Niu, Y. Feng, Q. Fu, S. Zhang, Y. Zhang, L. Li, X. Gu, P. Dai, D. Liu, Q. Zheng and X. Zhao, Adsorption in Reversed Order of C_2 Hydrocarbons on an Ultramicroporous Fluorinated Metal-Organic Framework, *Angew. Chem., Int. Ed.*, 2022, **61**, e202204046.
- 37 S.-M. Wang, H.-R. Liu, S.-T. Zheng, H.-L. Lan, Q.-Y. Yang and Y.-Z. Zheng, Control of pore structure by the solvent effect for efficient ethane/ethylene separation, *Sep. Purif. Technol.*, 2023, **304**, 122378.
- 38 E. Wu, X.-W. Gu, D. Liu, X. Zhang, H. Wu, W. Zhou, G. Qian and B. Li, Incorporation of multiple supramolecular binding sites into a robust MOF for benchmark one-step ethylene purification, *Nat. Commun.*, 2023, **14**, 6146.
- 39 M. H. Yu, H. Fang, H. L. Huang, M. Zhao, Z. Y. Su, H. X. Nie, Z. Chang and T. L. Hu, Tuning the Trade-Off between Ethane/Ethylene Selectivity and Adsorption Capacity within Isoreticular Microporous Metal-Organic Frameworks by Linker Fine-Fluorination, *Small*, 2023, **19**, 2300821.
- 40 R.-B. Lin, H. Wu, L. Li, X.-L. Tang, Z. Li, J. Gao, H. Cui, W. Zhou and B. Chen, Boosting Ethane/Ethylene Separation within Isoreticular Ultramicroporous Metal-Organic Frameworks, *J. Am. Chem. Soc.*, 2018, **140**, 12940–12946.
- 41 U. Böhme, B. Barth, C. Paula, A. Kuhnt, W. Schwieger, A. Mundstock, J. Caro and M. Hartmann, Ethene/Ethane and Propene/Propane Separation via the Olefin and Paraffin Selective Metal-Organic Framework Adsorbents CPO-27 and ZIF-8, *Langmuir*, 2013, **29**, 8592–8600.
- 42 Y. Ye, Y. Xie, Y. Shi, L. Gong, J. Phipps, A. M. Al-Enizi, A. Nafady, B. Chen and S. Ma, A Microporous Metal-Organic Framework with Unique Aromatic Pore Surfaces for High Performance C_2H_6/C_2H_4 Separation, *Angew. Chem., Int. Ed.*, 2023, **62**, e202302564.
- 43 H. Zeng, X.-J. Xie, M. Xie, Y.-L. Huang, D. Luo, T. Wang, Y. Zhao, W. Lu and D. Li, Cage-Interconnected Metal-Organic Framework with Tailored Apertures for Efficient C_2H_6/C_2H_4 Separation under Humid Conditions, *J. Am. Chem. Soc.*, 2019, **141**, 20390–20396.
- 44 O. T. Qazvini, R. Babarao, Z.-L. Shi, Y.-B. Zhang and S. G. Telfer, A Robust Ethane-Trapping Metal-Organic Framework with a High Capacity for Ethylene Purification, *J. Am. Chem. Soc.*, 2019, **141**, 5014–5020.
- 45 H. Wu, Y. Chen, D. Lv, R. Shi, Y. Chen, Z. Li and Q. Xia, An indium-based ethane-trapping MOF for efficient selective separation of C_2H_6/C_2H_4 mixture, *Sep. Purif. Technol.*, 2019, **212**, 51–56.
- 46 Y. Chen, H. Wu, D. Lv, R. Shi, Y. Chen, Q. Xia and Z. Li, Highly Adsorptive Separation of Ethane/Ethylene by An Ethane-Selective MOF MIL-142A, *Ind. Eng. Chem. Res.*, 2018, **57**, 4063–4069.

